Water Research 162 (2019) 358–368

Contents lists available at ScienceDirect

Water Research

journal homepage: www.elsevier.com/locate/watres

# Mutual benefits of acetate and mixed tungsten and molybdenum for their efficient removal in 40 L microbial electrolysis cells

Liping Huang [a, *], Fuping Tian [b], Yuzhen Pan [b], Liyuan Shan [a], Yong Shi [a], Bruce E. Logan [c]

[a] Key Laboratory of Industrial Ecology and Environmental Engineering, Ministry of Education (MOE), School of Environmental Science and Technology, Dalian University of Technology, Dalian, 116024, China
[b] College of Chemistry, Dalian University of Technology, Dalian, 116024, China
[c] Department of Civil and Environmental Engineering, The Pennsylvania State University, University Park, PA, 16802, USA

ARTICLE INFO

*Article history:*
Received 28 February 2019
Received in revised form
24 June 2019
Accepted 2 July 2019
Available online 4 July 2019

*Keywords:*
Scaled microbial electrolysis cell
Simultaneous removal of acetate
W(VI) and Mo(VI)
Bacterial community
Bioanode and biocathode

ABSTRACT

Practical application of metallurgical microbial electrolysis cells (MECs) requires efficient removal of metals and organics in larger reactors. A 40 L cylindrical single-chamber MEC fed acetate was used to achieve high removals of W(VI) and Mo(VI). In the presence of both metals, there were nearly complete removals of W (97 – 98%), Mo (98 – 99%), and acetate (95 – 96%), along with a low level of hydrogen production (0.0037–0.0039 L/L/d) at a hydraulic residence time (HRT) of 2 d (influent ratios of W:Mo:acetate of 0.5:1.0:24 mM). The final concentrations of these conditions were sufficient to meet national wastewater discharge standards. In the controls with individual metals or acetate, lower contaminant removals were obtained (W, 2 – 4%; Mo, 3 – 5%, acetate, 36 – 39%). Metals removal in all cases was primarily due to the biocathodes rather than the bioanodes. The presence of metals decreased microbial diversity on the anodes and increased diversity on the cathodes, based on analysis at the phylum, class and genus levels, as a function of HRT and influent concentration. This study demonstrated the feasibility of larger-scale single-chamber MECs for efficient treatment of W and Mo, moving metallurgical MECs closer to commercialization for wastewater treatment of these two metals.

© 2019 Elsevier Ltd. All rights reserved.

## 1. Introduction

Microbial electrolysis cells (MECs) have been intensively studied for achieving energy neutral organic wastewater treatment and accomplishing hydrogen production using a small applied voltage relative to that needed for splitting water (Logan et al., 2015; Jain and He, 2018). While scaled MECs for synthetic or practical urban wastewater treatment are still on-going (Luo et al., 2017; Rossi et al., 2019), the concept of microbial electro-metallurgy, or metals removals working under the overall principles of MECs or microbial fuel cells, has recently attracted a great deal of attention due to its multiple merits of recovery of metals, wastewater treatment of organic matter, and small energy consumption or net energy production (Abourached et al., 2014; Wang and Ren, 2014; Nancharaiah et al., 2016; Dominguez-Benetton et al., 2018). The most common configuration for metal-removal MECs consists of two chambers and a separator, where organics are oxidized by microbial anodes and metal ions are reduced to solid metals on abiotic cathodes. Many tests have been conducted using only one metal (Huang et al., 2013a; Jiang et al., 2014; Dominguez-Benetton et al., 2018), but many wastewaters often contain two or more metals. Thus, there have been other two-chamber MEC studies examining removals of two metals, for example V(V) and Cr(VI), Cu(II) and Cd(II), Cu(II) and Co(II), W(VI) and Mo(VI), three metals, such as Cr(VI), Cd(II) and Cu(II), Cu(II), Ni(II) and Fe(II), and Sn(II), Cu(II) and Fe(II), and four metals (Cu, Pb, Cd, and Zn), but all tests used small reactors (14 – 250 mL) (Modin et al., 2012; Zhang et al., 2012, 2015; Luo et al., 2014; Wu et al., 2016; Song et al., 2019). The use of two chambers and an ion exchange membrane increases capital costs, and limits practical applications for scale-up and commercialization (Abourached et al., 2014; Kadier et al., 2016; Rossi et al., 2019; Enzmann et al., 2019). Single-chamber configurations are therefore more attractive due to typically lower internal resistances, simpler architectures, and therefore more cost effective operation for simultaneous treatment of organics and metals (Abourached et al., 2014; Wu et al., 2018). However, single-chamber reactors have only been examined for metals removal that have small liquid volumes (12 – 28 mL), in tests using acetate and a

* Corresponding author.
*E-mail address:* lipinghuang@dlut.edu.cn (L. Huang).

https://doi.org/10.1016/j.watres.2019.07.003
0043-1354/© 2019 Elsevier Ltd. All rights reserved.

single metal in solution (Zn, Cd or Cu). It has been suggested that practical applications of MECs for metals removals will require demonstrations in reactors of 10 L or more (Enzmann et al., 2019).

The two transition metals tungsten (W) and molybdenum (Mo), are often concomitantly present in the leaching liquor of many spent industrial products and ore dressing wastewaters along with volatile fatty acids (Lasheen et al., 2015). Chemical, electrochemical or biological processes conventionally used for treating this wastewater involve the use of reducing agents, high energy consumption, or generation of large volumes of chemical sludge. Although abiotic removal of W and Mo has been demonstrated in smaller two-chamber MECs (Huang et al., 2017, 2018a; Wang et al., 2017, 2018; 2019a, 2019b), simultaneous organics treatment has not previously been examined in single-chamber systems, or at larger scales. Compact reactors are also needed for efficient treatment using MECs to minimize the potential for clogging (Rossi et al., 2019). Packing a high amount of electrode area per volume can be accomplished by using thin electrodes, such as graphite felt, and providing conductivity for larger electrodes using stainless steel mesh current collectors (Huang et al., 2010; Guo et al., 2017). Tubular or cylindrical MECs have been explored for hydrogen production in MECs at larger working volumes of 0.5–4 L (Gil-Carrera et al., 2013; Guo et al., 2017; Feng et al., 2018) but not for metals removals at these larger scales.

Larger-scale, cylindrical-shaped single-chamber MECs (40 L) were investigated for treatment of mixed organic, W(VI) and Mo(VI), under different hydraulic residence times (HRTs) and influent strengths. Mutual benefits of acetate, and mixed W(VI) and Mo(VI) for their efficient removals were for the first time observed, with the effluent accomplishing the national wastewater discharge standard, addressing the feasibility of the scaled single-chamber MECs for treatment of mixed acetate, W(VI) and Mo(VI). The roles of the bioanodes and the biocathodes in W(VI) and Mo(VI) reduction were clarified, based on the observation by a scanning electron microscope (SEM) equipped with an energy dispersive X ray spectrometer (EDS), the precipitant analysis by X-ray photoelectron spectroscopy (XPS), and the clarification of compositions of bacterial communities developed on the anodes and the cathodes under different HRTs and influent strengths.

## 2. Materials and methods

### 2.1. Reactor construction

The cylindrical single-chamber reactors (34 cm inner diameter, 45 cm high) were made of polyvinyl chloride (PVC) and constructed with concentric electrodes (Fig. 1). Graphite felt (1 cm thick; Sanye, Beijing, China) was used for both electrodes, with the inner cathode 18 cm in diameter and 40 cm high, and the outer anode 22 cm in diameter and 40 cm high, producing a working liquid volume of 38 L with no separator between the electrodes. The specific surface areas were 18 $m^2/m^3$ for the anode, and 22 $m^2/m^3$ for the cathode, based on the area-specific calculation based on the cylindrical geometry as $2r^{-1}$, where $r$ is the electrode radius (Logan et al., 2015). Stainless steel mesh (type 304 SS, McMaster-Carr, OH), used as both the current collector and to support the felt electrodes, was extended outside the chambers for connecting the electrodes to a power source (Leici, Shanghai, China) (Rossi et al., 2019; Song et al., 2019). Grooves were made on the bottom of the reactors to hold the edges of the stainless steel mesh, producing a distance of 1.0 cm between the edges of the electrodes. Before installation, the felt was pretreated as previously described (Huang et al., 2010, 2013b). Reference electrodes (Ag/AgCl electrode, 195 mV versus standard hydrogen electrode, SHE) were inserted around the top section of the reactor and close to either the anode or the cathode to obtain cathode and anode potentials individually, with all potentials reported here versus SHE. A small resistor of 10 Ω was installed in the circuit to measure current based on the voltage drop across the resistor, using an automatic data acquisition system (PISO-813, Hongge Co., Taiwan). The reactors were airtight and were equipped with sampling ports. Reactors were wrapped with aluminum foil to exclude light to avoid the growth of algae. The reactors were initially operated at fed-batch mode at room temperature ($22 \pm 3$ °C), after which the reactors was shifted to continuous flow operation.

### 2.2. Inoculation and operation

The MECs were inoculated with 500 mL of suspended bacteria from a 250 mL cylindrical single-chamber MEC at a food to microorganisms ratio of $0.87 \pm 0.13$ g COD/(g SS·d), and an equivalent volume of a nutrient solution containing trace elements (Huang et al., 2010). The reactors were then acclimated in fed-batch operation to a synthetic wastewater composed of W(VI) (0.5 mM), Mo(VI) (1.0 mM) and acetate (24 mM) with a COD of 1.5 g/L. The acclimation of the reactors was considered complete after two additional fed-batch cycles, based on reproducible electrode potentials over the cycle (3 – 4 days).

For continuous flow tests, different concentrations of W(VI), Mo(VI) and acetate were used, at ratios (mM/mM) of 0.5:1.0:24, 0.5:1.0:12, 0.3:0.6:12, 0.2:0.4:12, or 0.1:0.2:12, in a medium with additional trace elements (Huang et al., 2010). Concentrations in actual wastewaters can vary of large ranges of 0.05–10 mM for total metals, and 5.8–30 mM for total volatile organics (Lasheen et al., 2015). The influent pH was set to 3.0 and the solution conductivity to 3.0 mS/cm, which are typical for acidic wastewaters containing organics, W(VI) and Mo(VI) (Lasheen et al., 2015; Huang et al., 2018a). All reagents used were of analytical grade and the solutions were prepared in distilled water. After continuous sparging with ultra-pure nitrogen gas, the solutions were pumped (BT100-2J, Lange, China) into the MECs under closed circuit conditions (CCC) at flow rates to produce HRTs of 12 h (52.8 mL/min), 24 h (26.4 mL/min) or 48 h (13.2 mL/min).

Three controls were operated: operation of the reactors under open circuit conditions (OCCs), to examine metals and acetate removal in the absence of current; using only acetate or only metals to examine removals of these components along; and a smaller cylindrical single-chamber MECs (250 mL, with 44 $cm^2$ anode and 19 $cm^2$ cathode, with specific surface areas of 57 $m^2/m^3$ for the anode, and 133 $m^2/m^3$ for the cathode) at a ratio of W:Mo:acetate of 0.5:1.0:24 mM, and an HRT of 2 d, to study the impact of reactor size on performance.

### 2.3. Measurements and analyses

The influent and effluent concentrations of W(VI) and Mo(VI) were determined as described previously (Wang et al., 2017). Acetate was measured based on soluble chemical oxygen demands (CODs) calibrated with acetate using a high performance liquid chromatograph (HPLC, Agilent 1100). Removals were based on dividing the measured removals by the influent concentrations. Hydrogen produced in the headspaces of the MECs was collected using a gas collecting bag and periodically analyzed using a gas chromatograph (GC7900, Tianmei, Shanghai). Hydrogen production (L/L-d) was calculated on total hydrogen recovered normalized to the reactor working volume and operational time (d). An external voltage of 0.5 V was used during the entire operation period. All electrode potentials were collected using a data acquisition (PISO-813, Hongge Co., Taiwan). The influent and effluent pHs were measured using a pH probe and meter (PHS-3C, Leici,

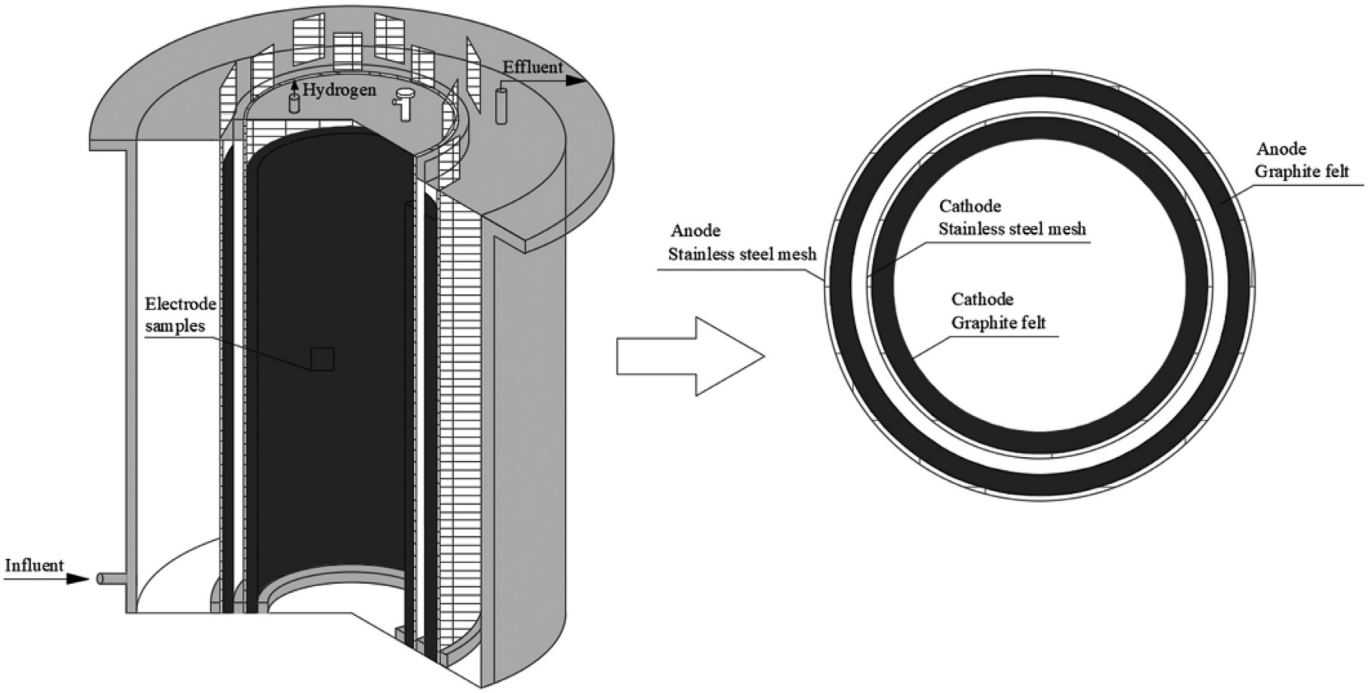


**Fig. 1.** The schematic of cylindrical single-chamber MEC reactor: (A) isometric view of the MEC reactor; (B) top view of electrode arrays.

Shanghai). The influent and effluent solution conductivities were determined with a conductivity probe and meter (DDS-307, Leici, Shanghai). Electrochemical impedance spectroscopy (EIS) was conducted using a potentiostat (VSP, BioLogic) as previously described (Zhang et al., 2015; Wu et al., 2016) and modified in SI.

After a 30-d continuous operation, the anodes and the cathodes were sampled in the middle of the electrodes. Biofilm morphology and precipitates on the cathodes and the anodes were examined using a SEM (Nova NanoSEM450, FEI company, USA) equipped with an EDS (X-MAX 20 $mm^2$/50 $mm^2$, Oxford Instruments, UK). Prior to observation, the electrodes were collected and treated as previously described (Huang et al., 2012). The valences of products on the cathodes and the anodes were confirmed using XPS (Kratos AXIS Ultra DLD).

### 2.4. Bacterial community analysis

Samples were collected from the anodes and the cathodes of the MECs at the end of experiments following different set conditions of HRTs or influent concentrations. Five pieces of graphite felt ($1 \times 1 \times 1$ $cm^3$) were removed from multiple locations in the middle of the electrodes and mixed together for analysis. Samples were then treated and analyzed as described in SI.

## 3. Results and discussion

### 3.1. Effect of HRT

Efficient removal of W(VI) (97 – 98%), Mo(VI) (98 – 99%) and acetate (95 – 96%) (Fig. 2A and B), with simultaneous hydrogen production rate (0.0037–0.0039 L/L-d) (Fig. 2B) were achieved using an HRT of 2 d and influent concentrations of W:Mo:acetate of 0.5:1.0:24 mM. These removals were much higher than those in the controls with circuit current in the presence of metals and absence of acetate (W, 2 – 4%; Mo, 3 – 5%) (Fig. 2A), and in the absence of metals with only acetate (COD removal of 36–39%), along with slightly lower hydrogen production rates (0.0030–0.0031 L/L/d) (Fig. 2B). There were increases in pH and conductivity consistent with circuit current and acetate consumption, with the largest changes in pH and solution conductivities occurring in the presence of acetate and both metals (Fig. 2C). In all cases there was relatively higher circuit currents and lower cathode potentials in the presence of acetate and both metals (Fig. 2D).

These results demonstrate the mutual benefits of having acetate and both W and Mo metals present for their removal in an MEC. The percentage of COD removal has been reported to be unaffected by the COD strength using domestic wastewaters, that do not contain high concentrations of metals (He et al., 2016). The key reason for a change in COD removal in the experiments here is therefore the presence of multiple electron acceptors (eg. W(VI) and Mo(VI)), which as reviewed by He et al. (2015), can largely contribute to system performance. Collectively, these results demonstrate the close correlation between the acetate and the metals, as well as the more feasibility of the scaled MECs for treating mixed acetate, W(VI) and Mo(VI) rather than the standalone acetate or the metals.

The final effluent concentrations (W, 2 – 3 mg/L; Mo, 1 – 2 mg/L; COD, 45 – 53 mg/L) were below national wastewater discharge limits for China (GB18918–2002 and GB21/1627-2008), implying that treatment using this MEC would produce effluents suitable to discharge into the environment. The specific metabolism of the microorganisms towards the removal of W(VI), Mo(VI) and acetate from solution with simultaneous hydrogen production in the scaled MECs was further evidenced by the absence of any by-products in the headspace (absence of methane) and in the effluent (absence of any other organics and negligible biomass).

The extent and rates of removals of metals and COD in the 40 L MEC (Fig. 2) was very similar to that in the smaller, 250 mL reactor at an HRT of 2 d (Fig. S1), demonstrating that using a larger MEC did not impact metals and acetate removals. Hydrogen production rates (0.0079–0.0082 L/L/d) in the small reactors, however, were about 2 times as large as that in the 40 L MEC, likely reflecting increased recoveries of hydrogen in the smaller reactors, consistent

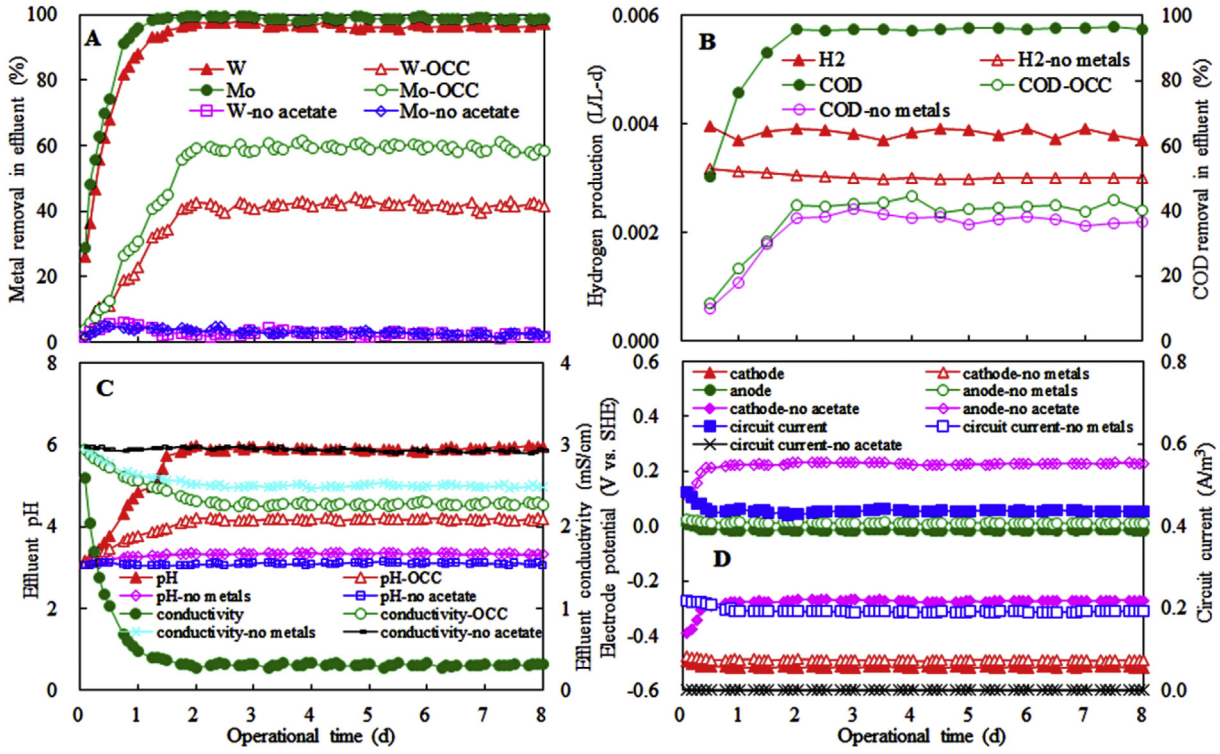


**Fig. 2.** (A) W and Mo removal, (B) COD removal and hydrogen production, (C) effluent pH and solution conductivity, and (D) electrode potential and circuit current in the presence of circuit current, or in the controls of open circuit conditions (OCC) or in the absence of either metals or organics (W:Mo:acetate = 0.5:1.0:24 mM, HRT: 2 d).

with other MEC reports showing reduced hydrogen gas recoveries with larger reactor sizes (Kadier et al., 2016; Logan et al., 2015). A lower hydrogen production in the 40 L MEC thus shows the compromise of the enlarged volume of reactor.

A shorter HRT of 1 d (Fig. 3), rather than 2 d (Fig. 2), reduced metals and acetate removals (W: 88 ± 1%, Mo: 94 ± 1%, COD: 73 ± 1%) (Fig. 3A and B), but slightly increased hydrogen production rates (0.0046 ± 0.0001 L/L-d) (Fig. 3B). This greater hydrogen rate may be related to the higher current density (0.61 ± 0.00 A/m$^3$) (Fig. 3D) since circuit current has been shown to be positively correlated with hydrogen production and negatively correlated with HRT in MECs (Lu and Ren, 2016; Kadier et al., 2016). The general trends in effluent pH, conductivity and electrode potentials (Fig. 3C and D) were similar to those observed with the 2 d HRT (Fig. 2). Less metals removal consumed less protons for oxometallate precipitates, resulting in lower effluent pHs and higher effluent conductivities (Fig. 3C) than those at 2 d (Fig. 2C).

### 3.2. Combined effect of influent strength and HRT

Lower in the acetate concentration to 12 mM (versus 24 mM), with the same HRT (1 d) and metal concentrations (W: Mo = 0.5 : 1.0), resulted in less metal removals and hydrogen production (Figs. S2A and B), but favored COD removal (Fig. S2B) (Fig. 3), consistent with the effluent pH and conductivity (Fig. S2C), and circuit current (Fig. S2D). In parallel, a shorter HRT (0.5 d) at a same strength influent (W:Mo:acetate = 0.5:1.0:12 mM), decreased metal and COD removal, and favored for hydrogen production (Fig. S2). These results illustrated the combined importance of organic strength and HRT for system performance.

Using a lower concentration of metals (W: 0.1–0.3 mM; Mo: 0.2–0.6 mM) at a 1 d HRT with the lower concentration of acetate (12 mM), produced higher metal removals (Fig. S3A). However, the lowest influent metals (W: 0.1 mM; Mo: 0.2 mM) resulted in the lowest COD removal and hydrogen production (Fig. S3B), consistent with the effluent pHs and solution conductivities (Fig. S3C) as well as the circuit currents (Fig. S3D). Collectively, these results illustrate the importance of appropriate ratios of metals and acetate in the influent for efficient system performance.

### 3.3. Continuous operation over 30 days at an HRT of 2 d

Operation of the 40 L MEC at a 2 d HRT showed that removal of metals (W: 94 – 96%; Mo: 95 – 99%) and COD (95 – 96%), circuit current and electrode potential were stable over 30 days of operation (Figs. S4A and C). The lower effluent conductivity was due to the change in effluent pH (Fig. S4B).

EIS spectra were fitted to equivalent circuits (Fig. S5) to identify the changes in the components of the internal resistances for the electrodes at the start of the tests and after 30 days (Fig. 4 and Table S1). There was only a small change in the ohmic resistances of the cathodes (23 Ω–28 Ω) and anodes (24 Ω–36 Ω), consistent with relatively small changes in solution conductivities. However, the charge transfer resistance nearly doubled for both electrodes (cathode, from 56 Ω to 105 Ω; anode, from 77 Ω to 142 Ω), suggesting a decay in electrode performance over time. These changes in resistance did not appear to impact overall reactor performance over the 30 d period. There were slight changes in the diffusion resistance that did not show any consistent change for both electrodes (cathode, from 83 Ω to 73 Ω; anode, from 52 Ω to 66 Ω). These results imply that changes in the electrochemical resistances did not substantially impact overall performance, but these changes do not readily reflect changes that could also be occurring in the microbial communities.

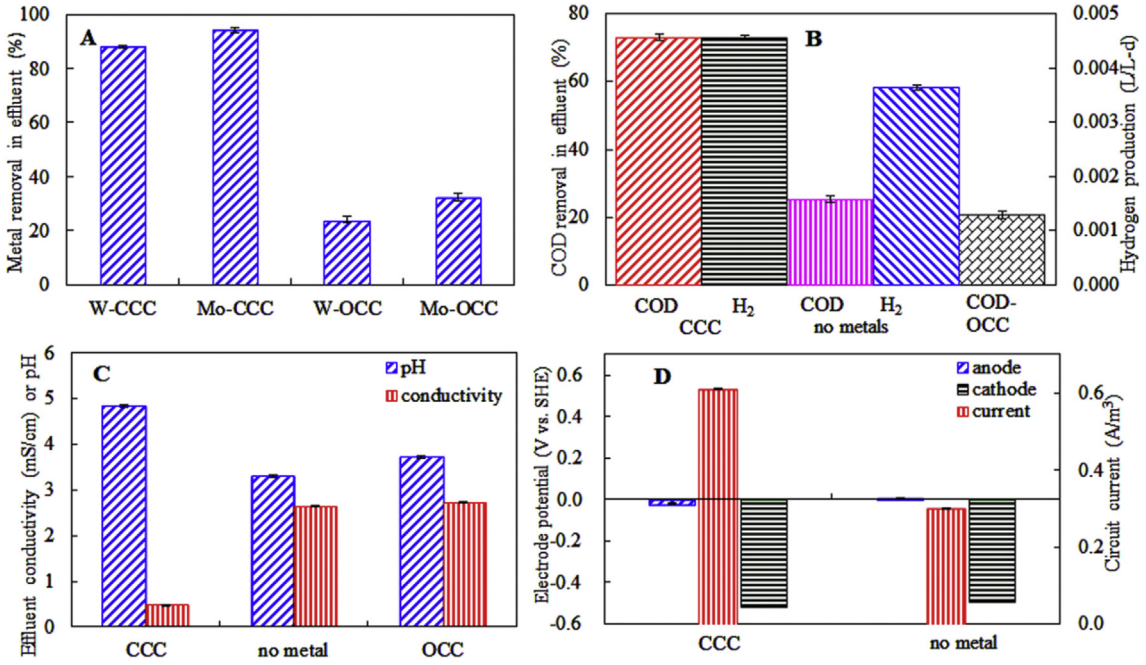


**Fig. 3.** (A) W and Mo removal, (B) COD removal and hydrogen production, (C) effluent pH and solution conductivity, and (D) electrode potential and circuit current at an HRT of 1 d (W:Mo:acetate = 0.5:1.0:24 mM).

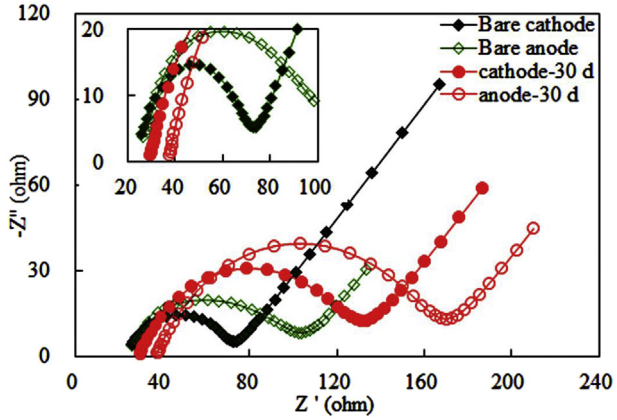


**Fig. 4.** Comparison of Nyquist plots of EIS spectra on the bare electrodes, and the cathodes and the anodes of the scaled MECs at the end of a 30-day operation (W(VI): Mo(VI): acetate = 0.5:1.0:24, HRT: 2 d).

### 3.4. Morphological observation of electrodes and analysis of metal precipitates

Cathodes and anodes were examined using SEM at the end of the continuous 30-day operation. Both the cathodes (Fig. 5A) and the anodes (Fig. 5C) were populated with bacteria and with noticeable precipitates on these bacterial surfaces. Relatively thick biofilms that developed on the anodes (Fig. 5C) were in contrast to the sparsely populated biofilms covering the cathodes (Fig. 5A). The sparser biofilms on the cathodes could have been caused by disruption and dislodging biofilm due to the evolution of hydrogen gas from the electrodes. However, sparsely populated biofilms have frequently been observed on cathodes with other terminal electron acceptors such as nitrate, oxygen or chlorophenols acceptors, even in the absence of hydrogen evolution (Huang et al., 2012, 2013b; Logan et al., 2019; Xie et al., 2011).

Analysis of the biofilm precipitates indicated reduction of W(VI) and Mo(VI) on bacterial cells on the anode, although to a lesser extent than that observed on the cathodes. The greater reduction of W(VI) and Mo(VI) on the cathodes was ascribed to the cathodic reductive environment, in agreement with the extensive literature on reduction of many other heavy metals on the cathodes of bio-electrochemical systems (Nancharaiah et al., 2016; Dominguez-Benetton et al., 2018). The observed reduction of W(VI) and Mo(VI) on the anodes is similarly supported by previous studies showing both anodic Cr(VI) reduction by *Ochrobactrum* sp. YC211 in dual-chamber microbial fuel cells (Chen et al., 2016), and the anodic Fe(III) reduction by predominant *Sphaerochaeta*, *Thermosinus*, *Arcobacter*, and *Hydrogenophage* in the anodic bacterial communities of single-chamber microbial fuel cells (Liu et al., 2018). Facultative anaerobic *Shewanella* sp., well known for their electrochemical activities in bioelectrochemical systems (Logan et al., 2019), have also been shown to use selenite as the sole electron acceptor for respiration under anaerobic conditions (Lee et al., 2007), similar to Cr(VI) reduction by many bacterial strains (Bachate et al., 2013; Banerjee et al., 2019; Thacker and Madamwar, 2005). Soluble and membrane-associated enzymes on the cellular surfaces of these bacteria have been proven to mediate the reduction of these metals (Thacker and Madamwar, 2005; Barrera-Diaza et al., 2012). Considering the fact of many bacteria such as *Raoultella ornithinolytica* Mo1, *Raoultella planticola* Mo1, *Pseudomonas* sp. DRY2, *Enterobacter* sp. Dr.Y13, or *Acinetobacter calcoaceticus* are capable of reducing Mo(VI) (Shukor et al., 2009, 2010a; 2010b; Saeed et al., 2019) and *Sulfitobacter dubius* NA4, As(V)4 and Sb5 for W(VI) reduction (Coimbra et al., 2017), the occurrence of W(VI) and Mo(VI) reduction on the bioanodes of the single-chamber MECs was not surprising.

Using EDS to examine the composition of the precipitates, stronger W and Mo signals were detected on the biocathodes (Fig. 5B) than on the bioanodes (Fig. 5D), with the amounts of W and Mo on the biocathodes 4.8 (W) and 4.2 (Mo) times of those on the bioanodes (Table S2). This again implies that most metals were reduced on the cathodes.

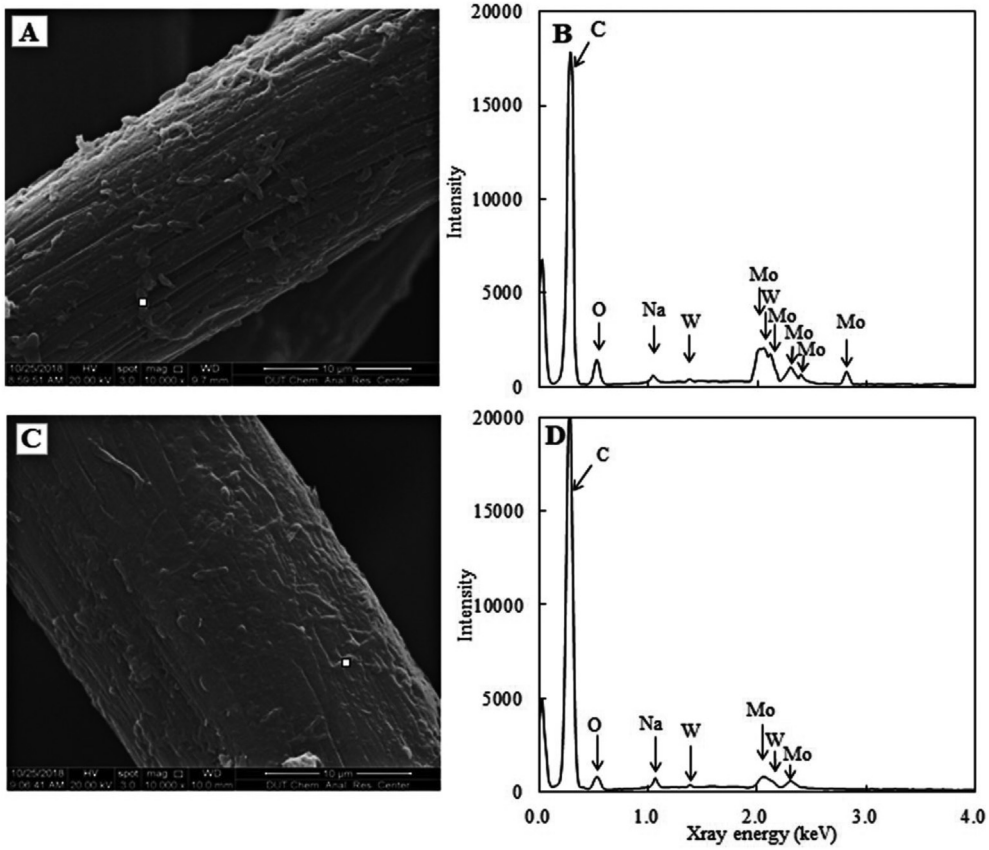


**Fig. 5.** (A and C) SEM and (B and D) EDS analysis on (A and B) the cathodes and (C and D) the anode of the system (W:Mo:acetate = 0.5:1.0:24, HRT: 2 d).

Biofilms formed can help to facilitate hydrogen production from the cathodes in MECs (Rozendal et al., 2008; Geelhoed and Stams, 2011). In the presence of electron acceptors of W(VI) and Mo(VI) in the electrolyte here, some of the in-situ generated hydrogen on the biocathodes could be used for the reduction of W(VI) and Mo(VI) (Wang et al., 2017, 2018; 2019a, 2019b), similar to other electron acceptors including nitrate, other metals, and carbon dioxide (Hou et al., 2018; Kadier et al., 2016; Nancharaiah et al., 2016; Xie et al., 2011). This reduction would explain the greater amounts of reduced precipitants on the biocathodes (Fig. 6A and C) than observed on the bioanodes (Fig. 6B and D).

XPS analysis of the cathodes indicated the presence of both W(V) and W(VI) (Fig. 6A), compared to only W(VI) on the anodes (Fig. 6B). This suggests that there was primarily W(VI) adsorption and precipitation on the anodes, while there was reduction of W on the cathode. In parallel, more Mo(VI), Mo(V) and Mo(IV) were simultaneously observed on the cathodes (Fig. 6C) than on the anodes (Fig. 6D), demonstrating greater Mo(VI) reduction on the cathodes. These higher XPS signals of reduced metals on the cathodes (Fig. 6A and C) than on the anodes (Fig. 6B and D), were consistent with the EDS results showing greater metal concentrations on the electrodes (Fig. 5B and D; Table S2).

The occurrence of some Mo(VI) reduction on the anodes implies Mo(VI) might compete with the anodes to accept electrons directly from the exoelectrogens, similar to many bacteria known to be capable of direct Mo(VI) reduction (Shukor et al., 2009, 2010a; 2010b; Lim et al., 2012; Othman et al., 2013), and mixed culture for Cd(II) or Zn(II) removal in single-chamber microbial fuel cells (Abourached et al., 2014). In the case of biocathodes, electron transfer from electrotrophs to metal ions is not well established (Nancharaiah et al., 2016). Very recently, Rowe et al. (2018) demonstrated that *Shewanella oneidensis* MR-1 on a cathode acquired energy for oxygen reduction. This respiratory process has important implications for understanding the biocathodes for W(VI) and Mo(VI) reduction in the present system and the cellular conversion of the cathodic electrons to the electrotrophs, despite that direct proofs for such mechanism is still needed.

### 3.5. Changes in bacterial communities

From 10 generated libraries, a total of 469,826 high-quality 16S rRNA gene sequences were obtained with an average length of 440 nucleotides (Table S3). These sequences were assigned into 4400 OTUs with a distance limit of 0.03. Though the rarefaction curves did not exhibit a plateau (Fig. S6), the Good's Coverage estimators indicate that the sizes of libraries were sufficient to cover the bacterial communities (Table S3).

Compared to the controls in the absence of metals, the presence of W(VI) and Mo(VI) consistently decreased the diversity of the microbial communities on the anodes and increased the diversity on the cathodes, as shown in the Shannon indices from 3.18 to 1.23 (anode) and 1.03 to 2.63 (cathode) (Fig. S7 and Table S3). Considering the more critical role of the cathode than the anode in system performance (He et al., 2015), this increased diversity on the biocathodes may have substantially contributed to the enhanced system performance for metals removals (Figs. 2 and 3). However, the decreased diversity of the biofilms on the anodes cannot exclude their potential critical roles in system performance since the bacterial ability to conduct current may not be the only or main reason for the predominance of high electrochemically active bacteria (Logan et al., 2019). This result was very similar to the responses of the microbial communities on the anodes and the cathodes of

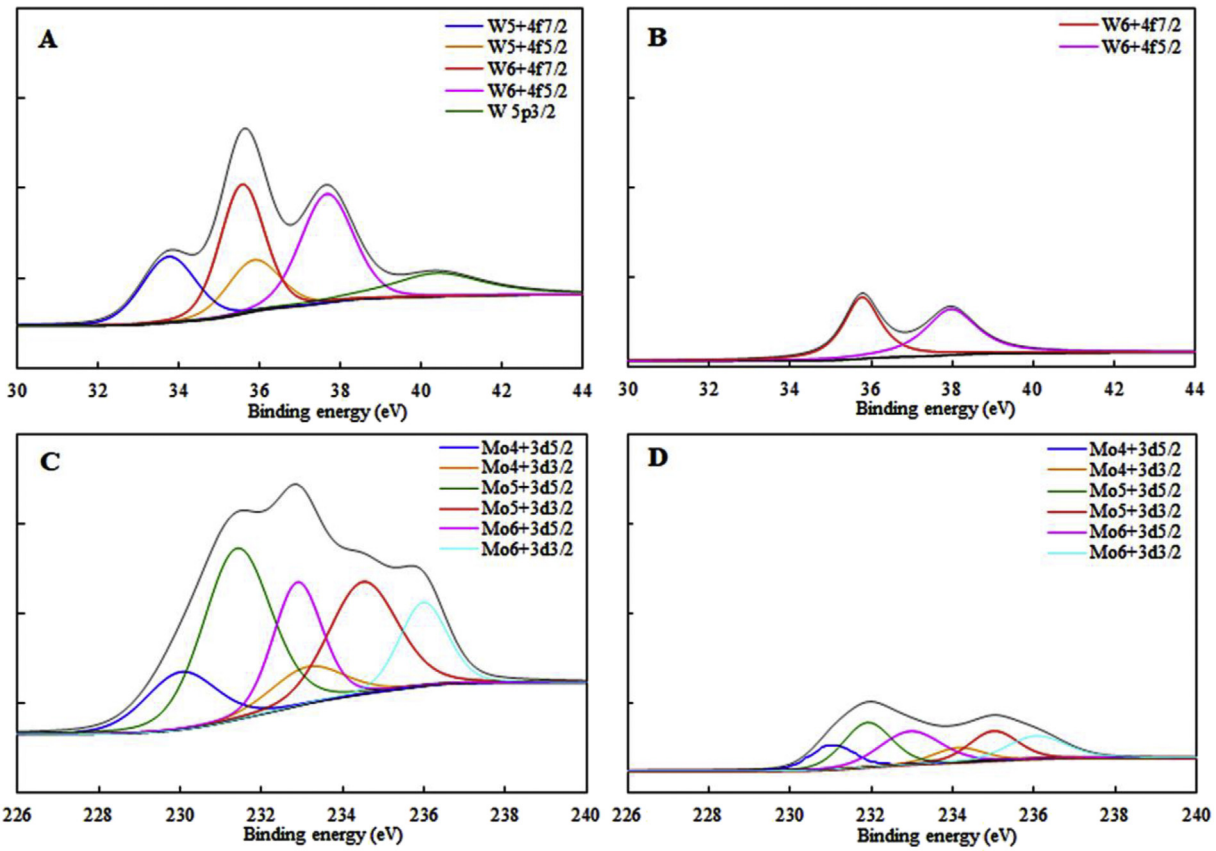


**Fig. 6.** XPS spectra of (A and B) W and (C and D) Mo precipitates on (A and C) the cathodes and (B and D) the anodes (W:Mo:acetate = 0.5:1.0:24, HRT: 2 d).

single-chamber microbial fuel cells to Fe(III), where the externally added Fe(III) shaped community structures of the electrode biofilms, resulting in the decreased (anode) and the increased (cathode) diversities of the microbial communities, compared to the controls in the absence of Fe(III) (Liu et al., 2018).

Analysis of the bacterial communities based on a Weighted Fast UniFrac Principle Coordinates Analysis indicated some general similarity in the communities acclimated to the different HRTs and concentrations of chemicals (Fig. 7A). The bioanodes and the biocathodes in the absence of metals, grouped in different quadrants. The presence of metals however, led to the more random dispersal of the anode than the cathode bacterial communities, particularly at shorter HRTs of 0.5 d or 1 d and regardless of the influent strength. A long HRT (2 d) and a high strength influent (W:Mo:acetate = 0.5:1.0:24 mM) led to a clustering of the different genus on both the anodes and the cathodes. A dendrogram constructed on the basis of community phylogenetic lineages further supported differences in these bacterial communities based on an absence of any close alignments of the communities at different HRTs and various strength influents (Fig. 7B). These findings illustrate that the compositions of the bacterial communities on the anodes and the cathodes were different from each other, and that a longer HRT (2 d) with a higher strength influent (W:Mo:acetate = 0.5:1.0:24) decreased the differences of the communities as they showed less dispersal.

The bacterial communities consisted of 5 phyla, with the majority of sequences (34.2–97.1%) belonging to *Proteobacteria* (Fig. 8A), which are frequently observed in bioelectrochemical systems (Lesnik and Liu, 2014; Logan et al., 2019). The presence of metals stimulated the relative abundance of *Proteobacteria* on the anodes (63.5–91.8%) and decreased them on the cathodes (78.6–88.3%), compared to those communities observed in the absence of metals (anode, 34.2%; cathode, 92.7%). Similarly, a low strength influent favored the abundance of *Proteobacteria* (anode, 91.8%; cathode, 88.3%), compared to those at a high strength influent (anode, 63.5%; cathode, 84.6%). A longer HRT of 2 d might have compensated for the higher strength influent, resulting in predominance of *Proteobacteria* (97.1%) on the cathodes, and *Proteobacteria* (82.7%) and *Firmicutes* (12.6%) on the anodes. The other *Actinobacteria* and *Bacteroidetes* apparently decreased in the presence of metals, and slightly changed with HRT and influent strength. Two classes (*Gamma-* and *Alpha-*) within *Proteobacteria* were predominantly observed from all communities, in addition to the minor *Betaproteobacteria* and *Deltaproteobacteria* (Fig. 8B).

Genus level analysis demonstrates a long HRT benefited an increased abundance of *Pseudomonas* and *Stenotrophomonas*, and diminished *Enterobacter* and *Desulfovibrio* on both electrodes (Fig. 8C). Similarly, a high strength influent shifted the genera to *Bacillus* (4.3%) and *Rhodococcus* (0.8%) on the cathodes, and *Paenibacillus* (4.1%), *Brevundimonas* (3.5%), *Staphylococcis* (2.5%) and *Rhodococcus* (1.8%) on the anodes. In addition, *Enterobacter* sp., *Stenotrophomonas*, *Brevundimonas* and unclassfied on the cathodes, and *Enterobacter* sp. and *Shewanella* on the anodes largely increased in response to the high strength influent. In the controls, the absence of metals led to the predominant *Pseudomonas* (83.7%) on the cathodes and the prevalent *Stenotrophomonas* (13.0%), *Paenibacillus* (25.0%), *Clostridium sensu stricto* (12%) and *Rhodococcus* (16.9%) on the anodes. Collectively, these results demonstrated the influence of HRT and influent strength on the anodic and cathodic genera, which changed along with the system performance (Figs. 2

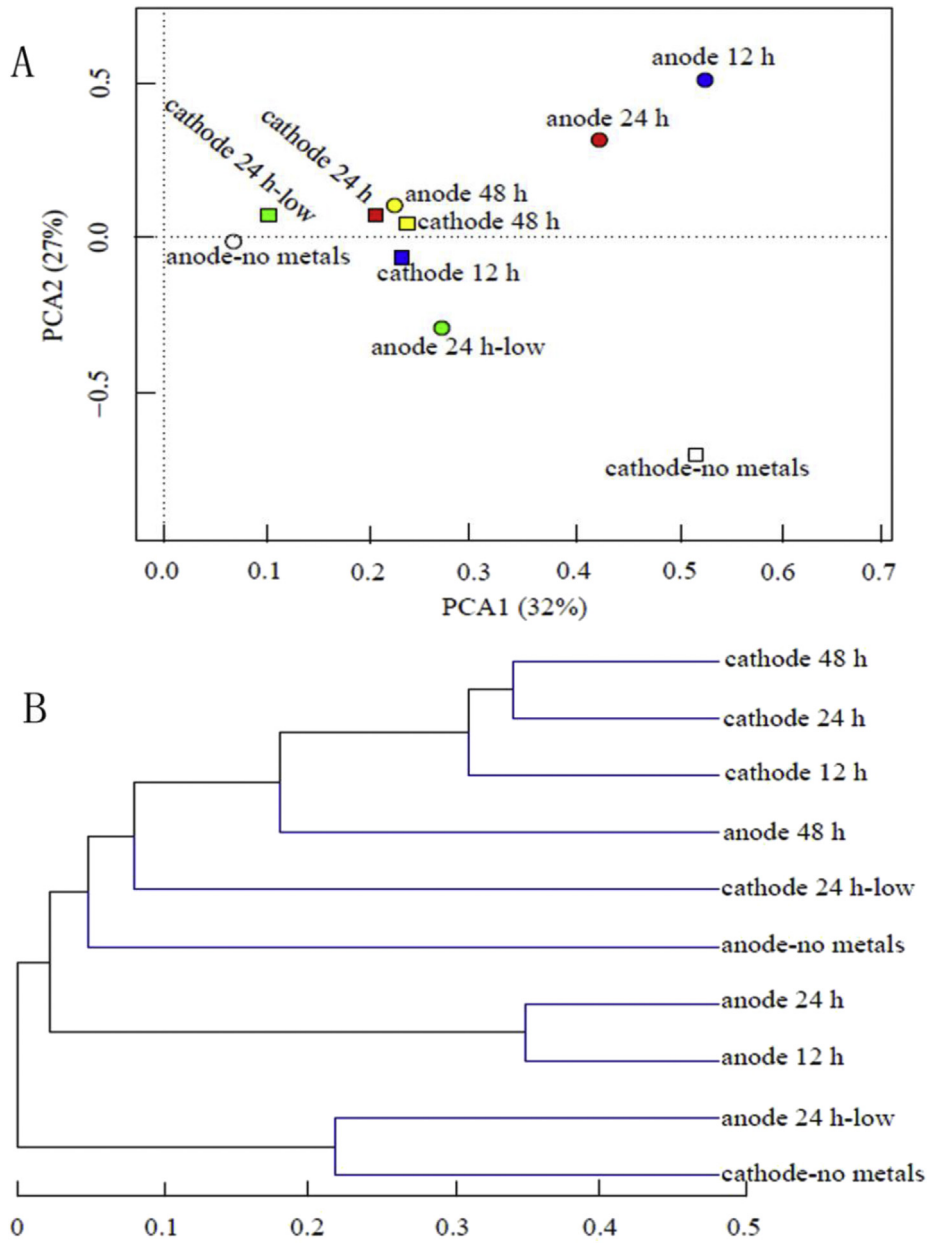


**Fig. 7.** Weighted Fast UniFrac (A) principle coordinates analysis and (B) cluster of the bacterial communities on the basis of phylogenetic lineages that samples contain.

and 3; Fig. S2 – 4).

Many bacteria including *Raoultella ornithinolytica*, *Raoultella planticola* (Saeed et al., 2019), *Bacillus amyloliquefaciens* (Maarof et al., 2018), *Pseudomonas* (Shukor et al., 2010a), *Enterobacter* (Shukor et al., 2009), *Klebsiella* (Lim et al., 2012), *Acinetobacter* (Shukor et al., 2010b), *Bacillus* sp. (Othman et al., 2013) and *Desulfovibrio desulfuricans* (Tucker et al., 1997) reportedly reduce Mo(VI) to Mo-blue in conventional biological processes. The observation of many of these genera in the 40 L MECs, thus implies their potential contribution to Mo(VI) reduction in these reactors. For tungsten, several W(VI)-tolerant strains including *Sulfitobacter dubius* NA4, As(V)4 and Sb5 reportedly grow and accumulate tungsten in the presence of a high W(VI) (1.0 mM) (Coimbra et al., 2017). Isolates with W(VI) and Mo(VI)-tolerant and electrochemically active characteristics from this system might enable to directly associate changes in biochemical metabolism and gene expression with the W(VI) and Mo(VI) reduction in the future investigation. At this time, however, it is only possible to infer the activities based on rDNA identification. Cytochrome profiling of pure cultures is helpful to examine whether differential expression of redox enzymes at the feeding of different influent strengths and various HRTs is a contributing factor to affect system performances. Studies on these genera, rather than studies confined to the model strains of *Geobacter* and *Shewanella* and some other isolates from single metal-removed bioelectrochemical systems (Huang et al., 2018a, 2018b; 2018c; Tao et al., 2017; Shen et al., 2017; Hou et al., 2018), will help us understand the roles of these genera in the bacterial community for complete and simultaneous removals of acetate, W(VI) and Mo(VI) in this system.

The different diversities of the microbial communities on the anodes and the cathodes in response to W(VI) and Mo(VI) might be related with the different behaviors of W(VI) and Mo(VI) on the anodes and the cathodes. Direct reduction of W(VI) and Mo(VI) competed with electron transfer to the anodes, and thus internally

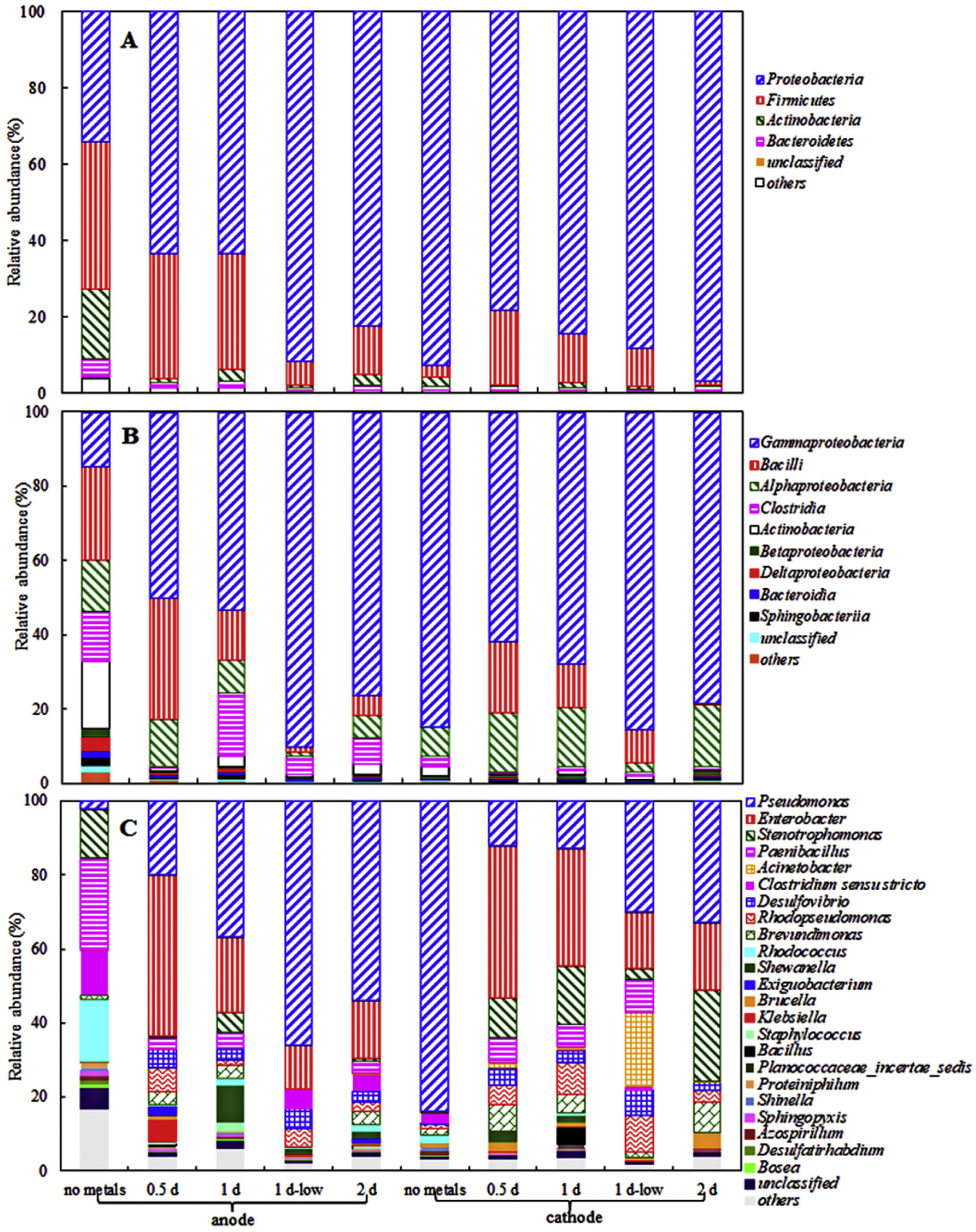


**Fig. 8.** Comparison of relative abundance of bacterial reads retrieved from the anodes and the cathodes under different conditions at the phylum level (A) and the class level distribution of the most dominant phylum of *Proteobacteria* (B). Phyla and classes that represent less than 1.0% of the total bacterial community composition were classified as "*others*". (no metals: no presence of metals, acetate 24 mM; 0.5 d or 1 d: HRTs of 0.5 d or 1 d, W:Mo:acetate = 0.5:1.0:24; 1 d-low: HRT of 1 d, W:Mo:acetate = 0.2:0.4:12; 2 d: HRT of 2 d, W:Mo:acetate = 0.5:1.0:24).

consumed electrons from exoelectrogens and negatively affected system performance in terms of circuit current. Conversely, W(VI) and Mo(VI) at the biocathodes could be used as terminal electron acceptors and thus may have benefited more diversified bacterial communities (He et al., 2015). Although tungstate or molybdate are key elements of coenzymes, and play key roles as enzyme activators in many bacteria (Hartmann et al., 2015; Saeed et al., 2019), the roles of W(VI) and Mo(VI) in the activities of bioanodes and the

biocathodes in single-chamber MECs, particularly at the molecular level, are largely unclear. A better understanding of the chemistry and biological transport in these systems will require the use of pure cultures to study gene expression.

The present study has illustrated the mutual benefits of acetate and mixed tungsten and molybdenum for their efficient removal in 40 L MECs, achieving nearly complete removals of W (97 – 98%), Mo (98 – 99%), and acetate (95 – 96%), compared to lower contaminant removals (W, 2 – 4%, Mo, 3 – 5%, acetate, 36 – 39%) in the controls with individual metals or acetate. An electron balance, based on the working volume of 38 L, showed that the total electrons required for reduction of W(VI) and Mo(VI) (0.11 mol) and hydrogen evolution (0.03 mol), and those from the oxidation of acetate (6.93–7.00 mol) were appreciably higher than the controls with individual metals (0.003–0.005 mol), hydrogen (0.02 mol) or acetate (2.63–2.85 mol). The ratio of electrons extracted from acetate and used for both W and Mo reduction, and hydrogen evolution was thus around 50, apparently lower than 114 in the controls with individual acetate or metals. This implies a better balance between acetate oxidation and mixed W and Mo reduction, and the more favorable result overall with using metals as more of the acetate was used when both metals were present, compared to individual metals or only electrons used for hydrogen production. This highlights the critical advantages of the mixed W, Mo and acetate over the individual components for efficient removal of these species in MECs, changing the general recognition on more efficient biological treatment efficiency for single rather than multiple contaminants in wastewaters (Lim et al., 2012; Lasheen et al., 2015). Overall, the presence of acetate improved W and Mo removal by 25–49 times and the presence of W and Mo together enhanced acetate removal by 2.5–2.7 times. Based on these encouraging results, this suggests that MECs could be superior to conventional biological processes for W and Mo removal from wastewater.

Compared to previous studies using small liquid volumes (12 – 28 mL) in single-chamber MECs for the removal of a single metals (Zn, Cd or Cu) (Abourached et al., 2014; Wu et al., 2018), the present study suggests the feasibility of larger-scale single-chamber MECs for efficient treatment of W and Mo, moving metallurgical MECs closer to commercialization for wastewater treatment of these two concomitant metals. Practical implementation will depend on the long-term operation of these reactors and other characteristics of the wastewaters, as well as the cost of the system relative to conventional treatment processes. At this point in time it is likely that this technology is not yet ready for commercial applications as even larger-scale studies would be required for evaluating the process prior to commercial and full scale applications.

## 4. Conclusions

- Simultaneous removal of acetate, and W and Mo was achieved in a 40 L cylindrical single-chamber MEC, with the effluent levels meeting national wastewater discharge standards for both metals and organics.
- The combination of acetate and the metals of W(VI) and Mo(VI) together had improved removals compared to acetate or metals alone.
- HRT and influent strength influenced the compositions of bacterial communities on the anodes and the cathodes, and may have contributed to system performance under different conditions.

## Conflicts of interest

There are no conflicts to declare.

## Acknowledgements

The authors gratefully acknowledge financial support from the National Natural Science Foundation of China (Nos. 51578104 and 21777017) and the Programme of Introducing Talents of Discipline to Universities (B13012).

## Appendix A. Supplementary data

Supplementary data to this article can be found online at https://doi.org/10.1016/j.watres.2019.07.003.

## References

Abourached, C., Catal, T., Liu, H., 2014. Efficacy of single-chamber microbial fuel cells for removal of cadmium and zinc with simultaneous electricity production. Water Res. 51, 228–233.
Bachate, S.P., Nandre, V.S., Ghatpande, N.S., Kodam, K.M., 2013. Simultaneous reduction of Cr(VI) and oxidation of As(III) by *Bacillus firmus* TE7 isolated from tannery effluent. Chemosphere 90, 2273–2278.
Banerjee, S., Misra, A., Chaudhury, S., Dam, B., 2019. A *Bacillus* strain TCL isolated from Jharia coalmine with remarkable stress responses, chromium reduction capability and bioremediation potential. J. Hazard Mater. 367, 215–223.
Barrera-Diaza, C.E., Lugo-Lugo, V., Bilyeu, B., 2012. A review of chemical, electrochemical and biological methods for aqueous Cr(VI) reduction. J. Hazard Mater. 223–224, 1–12.
Chen, C.Y., Cheng, C.Y., Chen, C.K., Hsieh, M.C., Lin, S.T., Ho, K.Y., Li, J.W., Lin, C.P., Chung, Y.C., 2016. Hexavalent chromium removal and bioelectricity generation by *Ochrobactrum* sp. YC211 under different oxygen conditions. J. Environ. Sci. Health A 51, 502–508.
Coimbra, C., Farias, P., Branco, R., Morais, P.V., 2017. Tungsten accumulation by highly tolerant marine hydrothermal Sulfitobacter dubius strains carrying a tupBCA cluster. Syst. Appl. Microbiol. 40, 388–395.
Dominguez-Benetton, X., Varia, J.C., Pozo, G., Modin, O., Ter Heijne, A., Fransaer, J., Rabaey, K., 2018. Metal recovery by microbial electro-metallurgy. Prog. Mater. Sci. 94, 435–461.
Enzmann, F., Mayer, F., Stöckl, M., Mangold, K.M., Hommel, R., Holtmann, D., 2019. Transferring bioelectrochemical processes from H-cells to a scalable bubble column reactor. Chem. Eng. Sci. 193, 133–143.
Feng, H., Huang, L., Wang, M., Xu, Y., Shen, D., Li, N., Chen, T., Guo, K., 2018. An effective method for hydrogen production in a single-chamber microbial electrolysis by negative pressure control. Int. J. Hydrogen Energy 43, 17556–17561.
Geelhoed, J.S., Stams, A.J.M., 2011. Electricity-assisted biological hydrogen production from acetate by *Geobacter sulfurreducens*. Environ. Sci. Technol. 45, 815–820.
Gil-Carrera, L., Escapa, A., Carracedo, B., Morán, A., Gómez, X., 2013. Performance of a semi-pilot tubular microbial electrolysis cell (MEC) under several hydraulic retention times and applied voltages. Bioresour. Technol. 146, 63–69.
Guo, K., Prévoteau, A., Rabaey, K., 2017. A novel tubular microbial electrolysis cell for high rate hydrogen production. J. Power Sources 356, 484–490.
Hartmann, T., Schwanhold, N., Leimkühler, S., 2015. Assembly and catalysis of molybdenum or tungsten-containing formate dehydrogenases from bacteria. BBA-Proteins Proteom 1854, 1090–1100.
He, C., Mu, Z., Yang, H., Wang, Y., Mu, Y., Yu, H., 2015. Electron acceptors for energy generation in microbial fuel cells fed with wastewaters: a mini-review. Chemosphere 140, 12–17.
He, W., Wallack, M.J., Kim, K.Y., Zhang, X., Yang, W., Zhu, X., Feng, C., Logan, B.E., 2016. The effect of flow modes and electrode combinations on the performance of a multiple module microbial fuel cell installed at wastewater treatment plant. Water Res. 105, 351–360.
Hou, X., Huang, L., Zhou, P., Xue, H., Li, N., 2018. Response of indigenous Cd-tolerant electrochemically active bacteria in MECs toward exotic Cr(VI) based on the sensing of fluorescence probes. Front. Environ. Sci. Eng. 12, 7.
Huang, L., Yang, X., Quan, X., Chen, J., Yang, F.L., 2010. A microbial fuel cell–electrooxidation system for coking wastewater treatment and bioelectricity generation. J. Chem. Technol. Biotechnol. 85, 621–627.
Huang, L., Gan, L., Wang, N., Quan, X., Logan, B.E., Chen, G., 2012. Mineralization of pentachlorophenol with enhanced degradation and power generation from air cathode microbial fuel cells. Biotechnol. Bioeng. 109, 2211–2221.
Huang, L., Li, T., Liu, C., Quan, X., Chen, L., Wang, A., Chen, G., 2013a. Synergetic interactions improve cobalt leaching from lithium cobalt oxide in microbial fuel cells. Bioresour. Technol. 128, 539–546.
Huang, L., Wang, Q., Quan, X., Liu, Y., Chen, G., 2013b. Bioanodes/biocathodes formed at optimal potentials enhance subsequent pentachlorophenol degradation and power generation from microbial fuel cells. Bioelectrochemistry 94, 13–22.
Huang, L., Li, M., Pan, Y., Shi, Y., Quan, X., Li Puma, G., 2017. Efficient W and Mo deposition and separation with simultaneous hydrogen production in stacked bioelectrochemical systems. Chem. Eng. J. 327, 584–596.
Huang, L., Li, M., Pan, Y., Quan, X., Yang, J., Li Puma, G., 2018a. Deposition and

separation of W and Mo from aqueous solutions with simultaneous hydrogen production in stacked bioelectrochemical systems (BESs): impact of heavy metals W(VI)/Mo(VI) molar ratio, initial pH and electrode material. J. Hazard Mater. 353, 348–359.
Huang, L., Xue, H., Zhou, Q., Zhou, P., Quan, X., 2018b. Imaging and distribution of Cd(II) ions in electrotrophs and its response to current and electron transfer inhibitor in microbial electrolysis cells. Sensor. Actuator. B Chem. 255, 244–254.
Huang, L., Zhou, P., Quan, X., Logan, B.E., 2018c. Removal of binary Cr(VI) and Cd(II) from the catholyte of MFCs and determining their fate in EAB using fluorescence proves. Bioelectrochemistry 122, 61–68.
Jain, A., He, Z., 2018. "NEW" resource recovery from wastewater using bioelectrochemical systems: moving forward with functions. Front. Environ. Sci. Eng. 12, 1.
Jiang, L., Huang, L., Sun, Y., 2014. Recovery of flakey cobalt from aqueous Co(II) with simultaneous hydrogen production in microbial electrolysis cells. Int. J. Hydrogen Energy 39, 654–663.
Kadier, A., Simayi, Y., Abdeshahian, P., Azman, N.F., Chandrasekhar, K., Kalil, M.S., 2016. A comprehensive review of microbial electrolysis cells (MEC) reactor designs and configurations for sustainable hydrogen gas production. Alex. Eng. J. 55, 427–443.
Lasheen, T.A., El-Ahmady, M.E., Hassib, H.B., Helal, A.S., 2015. Molybdenum metallurgy review: hydrometallurgical routes to recovery of molybdenum from ores and mineral raw materials. Miner. Process. Extr. Metall. Rev. 36, 145–173.
Lee, J.H., Han, J., Choi, H., Hur, H.G., 2007. Effects of temperature and dissolved oxygen on Se(IV) removal and Se(0) precipitation by *Shewanella* sp. HN-41. Chemosphere 68, 1898–1905.
Lesnik, K.L., Liu, H., 2014. Establishing a core microbiome in acetate-fed microbial fuel cells. Appl. Microbiol. Biotechnol. 98, 4187–4196.
Lim, H.K., Syed, M.A., Shukor, M.Y., 2012. Reduction of molybdate to molybdenum blue by *Klebsiella* sp. stain hkeem. J. Basic Microbiol. 52, 296–305.
Liu, Q., Yang, Y., Mei, X., Liu, B., Chen, C., Xing, D., 2018. Response of the microbial community structure of biofilms to ferric iron in microbial fuel cells. Sci. Total Environ. 631–632, 695–701.
Logan, B.E., Wallack, M.J., Kim, K.Y., He, W., Feng, Y., Saikaly, P.E., 2015. Assessment of microbial fuel cell configurations and power densities. Environ. Sci. Technol. Lett. 2, 206–214.
Logan, B.E., Rossi, R., Ragab, A., Saikaly, P.E., 2019. Electroactive microorganisms in bioelectrochemical systems. Nat. Rev. Microbiol. 17, 307–319.
Lu, L., Ren, Z., 2016. Microbial electrolysis cells for waste biorefinery: a state of the art review. Bioresour. Technol. 215, 254–264.
Luo, H., Liu, G., Zhang, R., Bai, Y., Fu, S., Hou, Y., 2014. Heavy metal recovery combined with $H_2$ production from artificial acid mine drainage using the microbial electrolysis cell. J. Hazard Mater. 270, 153–159.
Luo, S., Jain, A., Aguilera, A., He, Z., 2017. Effective control of biohythane composition through operational strategies in an innovative microbial electrolysis cell. Appl. Energy 206, 879–886.
Maarof, M.Z., Shukor, M.Y., Mohamad, O., Karamba, K.I., Halmi, M.I.E., Rahman, M.F.A., Yakasai, H.M., 2018. Isolation and characterization of a molybdenum-reducing *Bacillus amyloliquefaciens* strain KIK-12 in soils from Nigeria with the ability to grow on SDS. J. Environ. Microbiol. Toxicol. 6, 13–20.
Modin, O., Wang, X., Wu, X., Rauch, S., Fedje, K.K., 2012. Bioelectrochemical recovery of Cu, Pb, Cd, and Zn from dilute solutions. J. Hazard Mater. 235, 291–297.
Nancharaiah, Y.V., Venkata Mohan, S., Lens, P.N.L., 2016. Biological and bioelectrochemical recovery of critical and scarce metals. Trends Biotechnol. 34, 137–155.
Othman, A.R., Bakar, N.A., Halmi, M.I.E., Johari, W.L.W., Ahmad, S.A., Jirangon, H., Syed, M.A., Shukor, M.Y., 2013. Kinetics of molybdenum reduction to molybdenum blue by *Bacillus* sp. Strain A.rzi. BioMed. Res. Inter. 1–9, 2013.
Rossi, R., Jones, D., Myung, J., Zikmund, E., Yang, W., Gallego, Y.A., Pant, D., Evans, P.J., Page, M.A., Cropek, D.M., Logan, B.E., 2019. Evaluating a multi-panel air cathode through electrochemical and biotic tests. Water Res. 148, 51–59.
Rowe, A.R., Rajeev, P., Jain, A., Pirbadian, S., Okamoto, A., Gralnick, J.A., El-Naggar, M.Y., Nealson, K.H., 2018. Tracking electron uptake from a cathode into *Shewanella* cells: implications for energy acquisition from solid-substrate electron donors. mBio 9, e02203–e02217.
Rozendal, R.A., Jeremiasse, A.W., Hamelers, H.V.M., Buisman, C.J.N., 2008. Hydrogen production with a microbial biocathode. Environ. Sci. Technol. 42, 629–634.
Saeed, A.M., El Shatoury, E., Hadid, R., 2019. Production of molybdenum blue by two novel molydate-reducing bacteria belonging to the genus *Raoultella* isolated from Egypt and Iraq. J. Appl. Microbiol. 126, 1722–1728.
Shen, J., Huang, L., Zhou, P., Quan, X., Li Puma, G., 2017. Correlation between circuital current, Cu(II) reduction and cellular electron transfer in EAB isolated from Cu(II)-reduced biocathodes of microbial fuel cells. Bioelectrochemistry 114, 1–7.
Shukor, M.Y., Rahman, M.F., Shamaan, N.A., Syed, M.A., 2009. Reduction of molybdate to molybdenum blue by *Enterobacter* sp. strain Dr.Y13. J. Basic Microbiol. 49, S43–S54.
Shukor, M.Y., Ahmad, S.A., Nadzir, M.M.M., Abdullah, M.P., Shamaan, N.A., Syed, M.A., 2010a. Molybdate reduction by *Pseudomonas* sp. strain DRY2. J. Appl. Microbiol. 108, 2050–2058.
Shukor, M.Y., Rahman, M.F., Suhaili, Z., Shamaan, N.A., Syed, M.A., 2010b. Hexavalent molybdenum reduction to Mo-blue by *Acinetobacter calcoaceticus*. Folia Microbiol. 55, 137–143.
Song, X., Yang, W., Lin, Z., Huang, L., Quan, X., 2019. A loop of catholyte effluent feeding to bioanodes for complete recovery of Sn, Fe, and Cu with simultaneous treatment of the co-present organics in microbial fuel cells. Sci. Total Environ. 651, 1698–1708.
Tao, Y., Xue, H., Huang, L., Zhou, P., Yang, W., Quan, X., Yuan, J., 2017. Fluorescent probe based subcellular distribution of Cu(II) ions in living electrotrophs isolated from Cu(II)-reduced biocathodes of microbial fuel cells. Bioresour. Technol. 225, 316–325.
Thacker, U., Madamwar, D., 2005. Reduction of toxic chromium and partial localization of chromium reductase activity in bacterial isolate DM1. World J. Microbiol. Biotechnol. 21, 891–899.
Tucker, M.D., Barton, L.L., Thomson, B.M., 1997. Reduction and immobilization of molybdenum by *Desulfovibrio desulfuricans*. J. Environ. Qual. 26, 1146–1152.
Wang, H., Ren, Z., 2014. Bioelectrochemical metal recovery from wastewater: a review. Water Res. 66, 219–232.
Wang, Q., Huang, L., Quan, X., Zhao, Q., 2017. Preferable utilization of in-situ produced $H_2O_2$ rather than externally added for efficient deposition of tungsten and molybdenum in microbial fuel cells. Electrochim. Acta 247, 880–890.
Wang, Q., Huang, L., Quan, X., Zhao, Q., 2018. Cooperative light irradiation and in-situ produced $H_2O_2$ for efficient tungsten and molybdenum deposition in microbial electrolysis cells. J. Photochem. Photobiol. A Chem. 357, 156–167.
Wang, Q., Huang, L., Quan, X., Li Puma, G., 2019a. Sequential anaerobic and electro-Fenton processes mediated by W and Mo oxides for degradation/mineralization of azo dye methyl orange in photo assisted microbial fuel cells. Appl. Catal. B Environ. 245, 672–680.
Wang, Q., Cai, Z., Huang, L., Pan, Y., Quan, X., Li Puma, G., 2019b. Intensified degradation and mineralization of antibiotic metronidazole in photo-assisted microbial fuel cells with Mo-W catalytic cathodes under anaerobic or aerobic conditions in the presence of Fe(III). Chem. Eng. J. https://doi.org/10.1016/j.cej.2018.07.168.
Wu, D., Huang, L., Quan, X., Li Puma, G., 2016. Electricity generation and bivalent copper reduction as a function of operation time and cathode electrode material in microbial fuel cells. J. Power Sources 307, 705–714.
Wu, Y., Zhao, X., Jin, M., Li, Y., Li, S., Kong, F., Nan, J., Wang, A., 2018. Copper removal and microbial community analysis in single-chamber microbial fuel cell. Bioresour. Technol. 253, 372–377.
Xie, S., Liang, P., Chen, Y., Xia, X., Huang, X., 2011. Simultaneous carbon and nitrogen removal using an oxic/anoxic-biocathode microbial fuel cells coupled system. Bioresour. Technol. 102, 348–354.
Zhang, B., Feng, C., Ni, J., Zhang, J., Huang, W., 2012. Simultaneous reduction of vanadium (V) and chromium (VI) with enhanced energy recovery based on microbial fuel cell technology. J. Power Sources 204, 34–39.
Zhang, Y., Yu, L., Wu, D., Huang, L., Zhou, P., Quan, X., Chen, G., 2015. Dependency of simultaneous Cr(VI), Cu(II) and Cd(II) reduction on the cathodes of microbial electrolysis cells self-driven by microbial fuel cells. J. Power Sources 273, 1103–1113.